Rallis, Konstantinos G.; Papanikolaou, Vasilis K.; Diamantoulakis, Panagiotis D.; Tegos, Sotiris A.; Dowhuszko, Alexis A.; Khalighi, Mohammad Ali; Karagiannidis, George K.

Energy Efficient Cooperative Communications in Aggregated VLC/RF Networks with NOMA

Published in:
IEEE Transactions on Communications

DOI:
10.1109/TCOMM.2023.3292486

Published: 01/09/2023

Document Version
Peer-reviewed accepted author manuscript, also known as Final accepted manuscript or Post-print

Please cite the original version:
Rallis, K. G., Papanikolaou, V. K., Diamantoulakis, P. D., Tegos, S. A., Dowhuszko, A. A., Khalighi, M. A., & Karagiannidis, G. K. (2023). Energy Efficient Cooperative Communications in Aggregated VLC/RF Networks with NOMA. *IEEE Transactions on Communications*, *71*(9), 5408-5419. https://doi.org/10.1109/TCOMM.2023.3292486

Energy Efficient Cooperative Communications in Aggregated VLC/RF Networks with NOMA

Konstantinos G. Rallis, Vasilis K. Papanikolaou, *Member, IEEE*, Panagiotis D. Diamantoulakis, *Senior Member, IEEE*, Sotiris A. Tegos, *Member, IEEE*, Alexis A. Dowhuszko, *Senior Member, IEEE*, Mohammad-Ali Khalighi, *Senior Member, IEEE*, and George K. Karagiannidis, *Fellow, IEEE*

***Abstract*—Optimizing the energy efficiency (EE) of wireless networks is one of the key priorities in the design of beyond 5G mobile technologies. In this pursuit, the use of new frequency bands, in combination with advanced multiple access protocols and cooperative communications strategies, has recently shown promising results. To this end, this paper investigates an indoor wireless network that aggregates communication resources in visible light and radio-frequency (RF) bands, taking advantage of the complementary aspects of the two technologies. More specifically, a non-orthogonal multiple access (NOMA) scheme is introduced for the visible light communication (VLC) downlink, such that cell-edge users experiencing a weak VLC signal enhance their aggregated data rate with the aid of cooperative communications over RF sidelinks (i.e., device-to-device links). The optimal resource allocation strategy over both VLC and RF bands is derived aiming at EE maximization based on the Dinkelbach's algorithm and successive convex approximation. Additionally, for the sake of flexibility, a weighted EE metric is proposed for the characterization of the aggregated VLC/RF network performance. Simulation results are provided to validate the proposed analysis, revealing the impact of various design and system parameters, such as the weighting factors, quality of service requirements, and channel conditions.**

***Index Terms*—Visible light communications; Resource allocation; Energy efficiency; Aggregated VLC/RF networks; Cooperative NOMA; Sidelink communications.**

K. G. Rallis is with Wireless Communication and Information Processing (WCIP) group, Department of Electrical and Computer Engineering, Aristotle University of Thessaloniki, 54 124, Thessaloniki, Greece (e-mail: konralgeo@ece.auth.gr).

V. K. Papanikolaou is with the Institute for Digital Communications (IDC), Friedrich-Alexander-University Erlangen-Nuremberg (FAU), 91054 Erlangen, Germany (vpapanikk@ieee.org).

P. D. Diamantoulakis and S. A. Tegos are with the Department of Applied Informatics, University of Macedonia, 54636 Thessaloniki, Greece (e-mails: padiaman@ieee.org, sotiris.a.tegos@gmail.com).

A. Dowhuszko is with the Department of Information and Communications Engineering (DICE), Aalto University, 02150 Espoo, Finland (e-mail: alexis.dowhuszko@aalto.fi).

M.-A. Khalighi is with Aix-Marseille University, CNRS, Centrale Marseille, Institut Fresnel, Marseille, France (e-mail: ali.khalighi@fresnel.fr).

G. K. Karagiannidis is with the Wireless Communications & Information Processing (WCIP) group, Aristotle University of Thessaloniki, 54124 Thessaloniki, Greece and with the Cyber Security Systems and Applied AI Research Center, Lebanese American University (LAU), Lebanon (e-mail: geokarag@auth.gr).

This work was based upon work from European Union's Horizon 2020 COST Action CA19111 (European Network on Future Generation Optical Wireless Communication Technologies, NEWFOCUS).

The work of P. D. Diamantoulakis and S. A. Tegos was supported by the Hellenic Foundation for Research and Innovation (H.F.R.I.) under the "3rd Call for H.F.R.I. Research Projects to support Post-Doctoral Researchers" (Project Number: 7280).

The work of G. K. Karagiannidis was supported by the European Union's Horizon 2020 Research and Innovation Program under Agreement 957406.

This paper was presented in part at the 17th Int. Symp. Wireless Commun. Systems (ISWCS) [1].

I. INTRODUCTION

Conventional radio-frequency (RF) communications deal with the looming spectrum scarcity crisis due to the ever increasing number of devices requesting wireless connectivity, in particular in IoT applications, which also request for higher amounts of data traffic to be transported without a linear scaling on the energy that is consumed. More specifically, Ericsson forecasts that a smartphone's monthly usage will be about 35 GB by the end of 2026, and that majority of this mobile traffic will be generated indoors [2]. Moreover, according to Cisco [3], video devices will considerably increase as well, creating a multiplier effect on the data traffic to be supported by future mobile networks. To tackle this issue, academia and industry have shifted their attention to unexploited parts of the electromagnetic spectrum, especially in situations where connectivity issues may hinder the development of novel applications that will shape the landscape beyond 5G (B5G) [4].

Within this context, optical wireless communication (OWC) has been recently considered as a complementary technology to RF-only communication systems. More specifically, visible light communication (VLC), which uses the abundant and unlicensed bandwidth that is available in the visible spectrum, has shown potential to support a significant part of the new indoor traffic that will be generated B5G. In this sense, VLC is considered as a promising technology that makes use of light-emitting diodes (LEDs), as high energy-efficient light sources, to offer both communication and illumination services simultaneously. Other advantages of the VLC technology include the high physical layer security and the possibility of using a high frequency reuse factor, since visible light signals do not penetrate opaque objects such as walls. Nevertheless, since line-of-sight (LoS) can be easily interrupted by the movement or rotation of the user device, VLC networks can often experience link outages [5]. Since VLC does not interfere with RF signals [6], the study of wireless networks combining both technologies has become notably attractive due to their complementary benefits [7]. This constitutes the key idea behind hybrid cross-band VLC/RF wireless networks, which can be further categorized into *aggregated* and *non-aggregated* depending on how the communication resources are utilized [8]. In brief, in aggregated VLC/RF networks, information is received simultaneously over both bands, making decisions in a much faster scheduling time interval scale which resembles the carrier aggregation concept of 3GPP [9]. In contrast, non-aggregated VLC/RF networks use only one of these technologies in a much longer time scale, with the aid of a specific time switching mechanism that resembles a vertical handover operation between the two networks [9].

The interplay between VLC/RF technologies and other promising enablers of B5G wireless access, such as the use of non-orthogonal multiple access (NOMA), is critical for the improvement of key performance indicators (KPIs) related to the massive connectivity of devices and the spectral efficiency of point-to-point wireless links [10]. The advantages of NOMA, when compared to the conventional orthogonal multiple access schemes, have been demonstrated in several recent works [11], [12] and experimental studies [13], validating its use as a promising multiple access method for VLC networks. Note that specific degrees of freedom of VLC networks, such as the reception angle, can enhance the performance of NOMA even further. Meanwhile in the design of such schemes, energy efficiency (EE) should be considered as a critical criterion [14], as the network/device energy consumption per transmitted bit needs to be reduced due to both environmental and economic reasons [15].

A. State-of-the-Art

Recent papers have extensively investigated different approaches to improve the EE of hybrid cross-band VLC/RF networks. In particular, for non-aggregated VLC/RF networks, a plethora of use cases and scenarios have been considered so far in [15]–[19]. For example, in [15], the power consumption of a hybrid VLC/RF network was minimized while fulfilling the data rate request of users and maintaining the illumination level requirements. Moreover, in [16], the use of power line communication (PLC) backhauling for a hybrid VLC/RF system was considered, studying the optimal resource allocation to maximize the sum-data-rate of users under the assumption of both perfect and imperfect channel state information (CSI). The authors in [17] minimized the power consumption of both VLC and RF APs while verifying a target link outage probability constraint. Similarly, the data rate maximization of a VLC AP that provides simultaneously energy harvesting and RF relaying services to users in a cooperative fashion was considered in [18]. Also, cooperative hybrid VLC/RF systems with simultaneous lightwave information and power transfer (SLIPT) were studied in [19], where the authors proposed a cognitive-based resource allocation policy and introduced bounds for the harvested energy.

Although a number of works have also considered the design of aggregated VLC/RF networks, to the best of the authors' knowledge, they are not as extensively studied as the non-aggregated setups. For instance, the authors of [20] proved the non-surprising superiority of the aggregated over the non-aggregated approach in terms of the average system delay. Also, in a proof-of-concept experiment reported in [21], it was shown that the use of VLC/RF aggregation has potential to enable a three-fold gain on the average achievable throughput with respect to the client-server distance. When considering the use of a PLC backhaul for VLC APs, the authors of [22] optimized the resource allocation to maximize the EE of a PLC/VLC/RF network, whereas the authors in [23] defined a specific aggregated VLC/RF system based on cellular RF and VLC links to manage connectivity for outdoor and indoor users, respectively. Moreover, in [24], self-adaptive medium access control protocol was proposed to find a convenient trade-off between network delay, energy consumption, and probability of collision, while improving the overall data rate of the VLC/RF network. However, the considered solution was actually a non-aggregated VLC/RF network, since uplink and downlink were exclusively implemented over RF and VLC links respectively. On the other hand, [25], considered EE optimization for APs operating in both bands in the downlink, while in [26] a similar approach based on 802.11 MIMO was investigated for defining an aggregated VLC/RF network.

Regarding the utilization of NOMA for VLC, it has been extensively studied in the context of non-aggregated VLC/RF networks [27]–[32]. Specifically, aiming at solving the optimal user grouping problem, the use of coalitional game theory was considered in [27]. Moreover, the performance of a cooperative hybrid OWC/RF relay network with NOMA was examined in terms of outage probability in [29], utilizing for this purpose a cross-band selection diversity combining scheme to improve the overall system performance. In [30] and [31], power allocation and user pairing were further studied in a cooperative setup similar to the one in [29]. Also, in [32], cooperative diversity over RF links was utilized to improve the link reliability and to boost the outage performance of a NOMA-based VLC system. However, NOMA has not been investigated in the context of aggregated VLC/RF networks so far.

B. Motivation and Contribution

The aggregation of data rates in NOMA VLC systems with cooperative RF sidelink communications is crucial to capitalize the complementary advantages offered by these wireless technologies. When compared to non-aggregated VLC/RF systems, multi-link operation in a hybrid cross-band system using the aggregated approach can be utilized to provide more degrees of freedom to find a suitable trade-off between enhancing the data rate and improving the EE. It is important to highlight that the particularity of the proposed concept of aggregated VLC/RF networks here with respect to the literature, is that here the two wireless technologies are used simultaneously in every user's terminal. To this end, the main contributions of this work can be summarized as follows:

- Firstly, an aggregated transmission protocol is proposed based on VLC NOMA and cooperative RF (sidelink) communications. Here, the cell-center users act as decode-and-forward relays, receiving the information over the VLC link and forwarding part of it over an RF sidelink. Then, a cell-edge user can aggregate the information received over both VLC and RF links, enhancing hence its performance.
- A resource allocation problem is formulated aiming at maximizing the EE of the considered VLC/RF network using the proposed cooperative NOMA protocol, while fulfilling the quality of service (QoS) requirements of the users and taking into account the network power consumption constraints. The formulated problem is solved

using Dinkelbach's algorithm, the difference of convex (DC) structure of the resulting optimization problem, and successive convex approximation (SCA).
- Simulation results are presented to prove the superiority of the proposed cooperative NOMA protocol versus benchmarks that do not use NOMA and/or cooperative sidelink communications. Moreover, the effect of the weights of the EE and the RF channel is investigated, while the utilization of the RF link is examined for different user requirements and RF channel quality.

C. Paper Structure

The rest of the paper is organized as follows: Section II presents the system model and the formulas that have been selected to model the achievable data rate on both VLC and RF links. Section III proposes the aggregated VLC/RF protocol based on VLC NOMA and RF sidelink. Section IV derives the algorithm to optimize the EE of the proposed cooperative NOMA protocol, whereas Section V presents the numerical results with their detailed interpretation. Finally, conclusions are drawn in Section VI.

II. System Model

The system model for the hybrid VLC/RF downlink network is shown in Fig. 1 and consists of one VLC-AP and two users U_1 and U_2. Without loss of generality, the VLC-AP is placed at a height of L with respect to the height of the users, and user U_1 (cell-center user) is closer to the VLC-AP when compared to U_2. The location of user with index i is described by polar coordinates (ρ_i, ω_i), where ρ_i is the distance from the reference point and ω_i is the angle from the reference direction. Without loss of generality, the reference point is in the horizontal plane that contains both U_1 and U_2, just below the VLC-AP, and the reference direction points north on the same horizontal plane.

The position of U_1 is uniformly distributed on a circular disk of radius R_0, whereas the position of U_2 is uniformly distributed on an annular area bounded by inner radius R_0 and outer radius R_v, respectively. The VLC-AP uses NOMA to handle simultaneous data transmission to both users. To improve the data rate of cell-edge user U_2, cell-center user U_1 further acts as a decode-and-forward (DF) cooperative relay, receiving information on the VLC downlink and forwarding it to the final destination over an RF sidelink.

It should be highlighted that the proposed system model can be extended to the case of more than two users. However, this may increase the computational complexity of perform successive interference cancellation (SIC) at the receiver, which is prone to error propagation in the signal detection stages. To address this, user pairing can be used instead where the network provides wireless to more than two users at the same time by grouping one cell-center and one cell-edge user using an orthogonal multiple access (OMA). Note that since the size of a VLC cell is relatively small (on the order of a few meters), only few users will participate in the pairing process described above. In addition, as the number of users participating in the scheme increases, the gain of NOMA in terms of sum data rate decreases more and more.

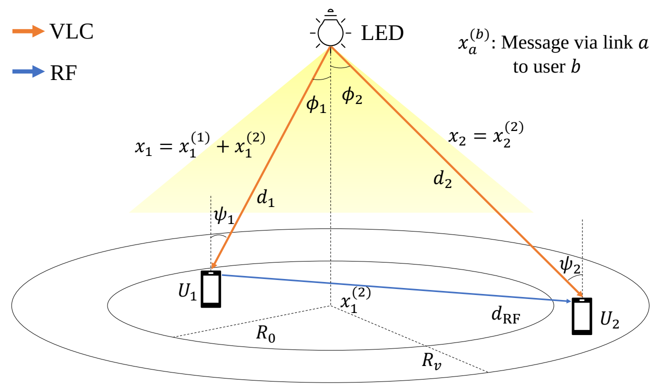

Fig. 1. System model to implement the proposed cooperative VLC NOMA protocol. Cell-center user (U_1) performs SIC to recover its own message and the message to be forwarded over the RF sidelink. Cell-edge user (U_2) aggregates the data rate from its own VLC reception (no SIC) and the sidelink communication.

A. VLC NOMA Transmission

We consider that intensity modulation and direct detection (IM/DD) is used with NOMA signaling over the VLC downlink. In this situation, the transmitted signal is given as

$$x = P_1\, x_1 + P_2\, x_2, \tag{1}$$

where P_1, P_2 are the transmitted optical powers allocated to U_1 and U_2, respectively, and x_1, x_2 are the corresponding messages. To maintain illumination levels while verifying eye safety and hardware constraints, the maximum transmitted optical power is limited to $P_{\max}^{\text{VLC}}$, i.e.,

$$P_1 + P_2 \leq P_{\max}^{\text{VLC}}. \tag{2}$$

Then, the received message at user U_i can be expressed as

$$y_i = \eta_{\text{PD}}\, h_i\, x + n_i, \qquad i = 1, 2, \tag{3}$$

where η_{PD} is the photodetector (PD) responsivity, h_i is the DC-gain of the VLC channel from the AP and the user with index i, and n_i is additive white Gaussian noise (AWGN). Assuming a LoS condition in the VLC link, we have that

$$h_i = \frac{m+1}{2\pi\, d_i^2} A_{\text{PD}} \cos^m(\phi_i)\, T(\psi_i)\, g(\psi_i)\, \cos(\psi_i), \tag{4}$$

where A_{PD} is the sensitive area of the PD (which is the same for both users), ϕ_i and ψ_i denote the irradiance and the incidence angles for user U_i, respectively (see Fig. 1), while m is the Lambertian emission order, which is defined as

$$m = -\ln(2)/\ln\big(\cos(\Phi_{1/2})\big), \tag{5}$$

where $\Phi_{1/2}$ being the transmitter semi-angle at half-power. The distance between AP and user U_i is given by $d_i = \sqrt{\rho_i^2 + L^2}$, where ρ_i is the radial coordinate of the user and L is the height at which the VLC-AP is placed. $T(\psi_i)$ and $g(\psi_i)$ denote the gains of the optical filter and the optical concentrator, respectively, i.e.,

$$g(\psi_i) = \begin{cases} \frac{\nu^2}{\sin^2 \Psi_{\text{FoV}}}, & 0 \leq \psi_i \leq \Psi_{\text{FoV}} \\ 0, & \psi_i > \Psi_{\text{FoV}} \end{cases}, \tag{6}$$

where $\Psi_{\rm FoV}$ denotes the field-of-view (FoV) of the PD placed at the VLC receiver and ν is the refractive index of its lens.

Without loss of generality, we assume that the PD of each user is pointing upwards, verifying $\phi_i = \psi_i$. Then, using polar coordinates to represent distances, the VLC channel gain from the AP to the user U_i becomes

$$h_i = \frac{(m+1)\, C_i\, L^{m+1}}{(\rho_i^2 + L^2)^{\frac{m+3}{2}}}, \qquad C_i = \frac{A_r T(\psi_i) g(\psi_i)}{2\pi}. \quad (7)$$

According to the power domain NOMA principle, the cell-edge user U_2 decodes its own message with an achievable data rate R_2^V by treating the message for U_1 as noise. At the cell-center user U_1, where the received VLC signal is stronger, the message of U_2 is first decoded and removed via SIC. Here, the rate at which user U_1 can decode the message intended to user U_2 is denoted by $R_{2\to 1}^V$. Following this, U_1 decodes its own message without interference with an achievable data rate equal to R_1^V. Due to IM/DD is utilized in the downlink direction, the standard Shannon formula cannot be used to evaluate the channel capacity since there are additional constraints to be verified, such as the non-negativity of the transmitted signal and the constraint on the maximum optical transmit power emitted by the LED. Instead, using a lower bound of the corresponding capacity region, the corresponding maximum achievable rates are given by [33]

$$R_{2\to 1}^V = B_v \log_2\left(1 + \frac{(\eta h_1 P_2)^2}{\left((\eta h_1 P_1)^2 + 9\sigma^2\right)\left(1+\epsilon_\mu\right)^2}\right) - \epsilon_\phi, \quad (8)$$

$$R_1^V = B_v \log_2\left(1 + \frac{(\eta h_1 P_1)^2}{9\sigma^2 (1+\epsilon_\mu)^2}\right) - \epsilon_\phi, \quad (9)$$

$$R_2^V = B_v \log_2\left(1 + \frac{(\eta h_2 P_2)^2}{\left((\eta h_2 P_1)^2 + 9\sigma^2\right)(1+\epsilon_\mu)^2}\right) - \epsilon_\phi, \quad (10)$$

where B_v is the electrical bandwidth of the VLC signal, σ^2 is the noise variance, and $\epsilon_\phi = 0.016$, $\epsilon_\mu = 0.0015$.

B. Sidelink RF Transmission

During RF transmission, the baseband equivalent received signal at cell-edge user U_2 is given by

$$y_R = \sqrt{L_{\rm RF} P_{\rm RF}}\, h_{\rm RF}\, x_R + n_R, \quad (11)$$

where $L_{\rm RF}$, $P_{\rm RF}$, x_R and n_R denote the path loss attenuation, the available RF power for retransmission at user U_1, the transmitted signal intended to user U_2, and the instantaneous noise at the RF receiver of U_2, which is statistically modeled as AWGN with zero mean and variance σ_R^2, respectively. Without loss of generality, we consider a Rician fading model for the fast-fading coefficient of the RF sidelink channel $h_{\rm RF}$, which follows the Rice distribution with parameters K_r, denoting the ratio of the power of the LoS component to that of the multipath reflections received through non-LoS propagation, and Ω, denoting the total sum received power from LoS and non-LoS components.

Given the considered scenario and using the polar coordinates for the positions of users U_1 and U_2, the Euclidean distance between the two users can be calculated as

$$d_{\rm RF} = \sqrt{\rho_1^2 + \rho_2^2 - 2\rho_1\rho_2 \cos(\theta_2 - \theta_1)}, \quad (12)$$

where θ_1 and θ_2 are the angular coordinates for the positions of users U_1 and U_2, respectively. Regarding the path loss attenuation, we consider the formula $L_{\rm RF}^{\rm dB} = L_{d_0}^{\rm dB} - 10\zeta \log_{10}(\frac{d_{\rm RF}}{d_0})$ which gives the value of the attenuation in dB, where ζ is the path loss exponent, and $L_{d_0}^{\rm dB} = -68\,{\rm dB}$ is the attenuation at the reference distance $d_0 = 1\,{\rm m}$ [34]. Then, using the Shannon capacity formula, the achievable data rate for the RF sidelink from user U_1 to user U_2 is given by

$$R_2^{\rm RF} = B_{\rm RF} \log_2\left(1 + \frac{L_{\rm RF} P_{\rm RF} |h_{\rm RF}|^2}{\sigma_R^2}\right), \quad (13)$$

where $B_{\rm RF}$ denotes the bandwidth of the RF signal.

III. Proposed Protocol for VLC/RF Aggregation

In this section, we propose an aggregated VLC/RF protocol based on VLC NOMA and RF sidelink communications. As it can be seen from (1) and Fig. 1, the VLC AP transmits the signal x, which contains x_1 and x_2. We assume that x_1 is the sum of U_1's desired information $x_1^{(1)}$ and a part of U_2's desired information denoted by $x_1^{(2)}$, whereas x_2 contains a different part of U_2's desired information denoted by $x_2^{(2)}$. We note that the way that $x_1^{(1)}$ and $x_1^{(2)}$ are separated at the cell-center user U_1 can be predefined and signaled from VLC AP to U_1. For instance, $x_1^{(1)}$ and $x_1^{(2)}$ can be aggregated frames obtained from x_1. It should also be highlighted that $x_1^{(2)}$ is independent from both $x_1^{(1)}$ and $x_2^{(2)}$, thus, cell-edge user U_2 does not utilize selection combining scheme as in [1], but needs to receive both $x_1^{(2)}$ and $x_2^{(2)}$ in an aggregated VLC-RF signal. To this end, the messages in the proposed protocol are given as

$$x_1 = x_1^{(1)} + x_1^{(2)}, \quad (14a)$$

$$x_2 = x_2^{(2)}. \quad (14b)$$

With the assumption of point-to-point communication and the independence of messages $x_1^{(1)}$ and $x_1^{(2)}$, the inequality

$$R_1^{(1)} + R_1^{(2)} \le R_1^V \quad (15)$$

on the data rate of the VLC link of user U_1 can defined, where $R_1^{(1)}$ and $R_1^{(2)}$ denote the achievable data rates of $x_1^{(1)}$ and $x_1^{(2)}$, respectively. After decoding x_1, U_1 separates $x_1^{(1)}$ and $x_1^{(2)}$, forwarding the latter part over the RF sidelink to U_2. Therefore, $x_1^{(2)}$ is relayed using the decode-and-forward protocol and it should stand that

$$R_1^{(2)} \le R_2^{\rm RF}, \quad (16)$$

where $R_2^{\rm RF}$ is the channel capacity of the RF sidelink. Finally, cell-edge user U_2 receives its desired information, represented by $x_2^{(2)}$ and $x_1^{(2)}$, via the VLC NOMA link and the RF sidelink, respectively. As stated in [35], the channel capacity of an aggregated VLC/RF system is unknown, but we can obtain a lower bound for it. Considering that (10) is a lower bound for the VLC channel capacity when the input signal values follow the truncated Gaussian distribution, and that (13) is the standard Shannon capacity formula when the values of the input signal follows the normalized complex Gaussian distribution, denoted by $\mathcal{CN}(0,1)$, we can write

$$R_2 = R_2^{\mathrm{RF}} + R_2^V. \tag{17}$$

Then, when the aim is to verify the QoS requirement for cell-edge user U_2, denoted by R_2^{thr}, the following inequality to be verified arises when combining (16) with (17):

$$R_1^{(2)} + R_2^V \geq R_2^{\mathrm{thr}}. \tag{18}$$

Finally, the QoS requirement for cell-center user U_1, which is denoted by R_1^{thr}, the following inequality must be hold

$$R_1^{(1)} \geq R_1^{\mathrm{thr}}. \tag{19}$$

Special Case: Non-aggregated VLC/RF Combining

As a special case to the aforementioned protocol, a simple selection combining can be considered when either the pure VLC-NOMA mode is used without RF sidelink communication or mixed VLC/RF mode. In this special case, either U_2's message is transmitted by the AP via the NOMA VLC method, or it is decoded and relayed by U_1 via the RF sidelink. This way, the message x_1 is not split and (18) becomes

$$qR_2^{\mathrm{RF}} + (1-q)R_2^V \geq R_2^{\mathrm{thr}} \tag{20}$$

with

$$q = \begin{cases} 0, & \text{for pure VLC-NOMA mode,} \\ 1, & \text{for mixed VLC/RF mode.} \end{cases} \tag{21}$$

It is noted that in the mixed VLC/RF mode, U_1 decodes U_2's message with achievable data rate $R_{2\to1}^V$, since power domain NOMA is used, thus it should stand that

$$R_{2\to1}^V \geq R_2^{\mathrm{thr}}. \tag{22}$$

IV. Energy Efficiency Optimization

Here, we first define the EE of the target VLC/RF network and then investigate the resource allocation problem that maximizes it. In fact, EE expresses how effectively the available power is utilized to achieve the desired transmission data rates, and is measured in bps/Hz/W. Thus, EE can be defined as the ratio of the spectral efficiency to the total consumed power. We consider two weighting coefficients, $\alpha \in [0,1]$ and $\beta \in [0,1]$, which assist in adapting EE to different scenarios. This way, the weighted EE metric can be expressed as

$$\mathcal{E} = \frac{\alpha R_1^{(1)} + (1-\alpha)\left(R_1^{(2)} + R_2^V\right)}{\beta P_{\mathrm{LED}} + (1-\beta)P_{\mathrm{RF}}}, \tag{23}$$

where $P_{\mathrm{LED}} = P_1 + P_2$, α is used to prioritize the users data rates, and β is used to focus on a specific power source.

Taking into account the QoS requirements for both users, which are given by (18) and (19), and the expressions for the achievable data rates, as well as the hardware and illumination constraints described in the previous section, we can write the EE optimization problem as follows:

$$\begin{aligned} \max_{P_1,P_2,P_{\mathrm{RF}},R_1^{(1)},R_1^{(2)}} \quad & \frac{\alpha R_1^{(1)} + (1-\alpha)\left(R_1^{(2)} + R_2^V\right)}{\beta P_{\mathrm{LED}} + (1-\beta)P_{\mathrm{RF}}} \\ \text{s.t.} \quad & \mathrm{C}_1: R_1^{(1)} \geq R_1^{\mathrm{thr}}, \\ & \mathrm{C}_2: R_1^{(2)} + R_2^V \geq R_2^{\mathrm{thr}}, \\ & \mathrm{C}_3: R_1^{(2)} \leq R_2^{\mathrm{RF}}, \\ & \mathrm{C}_4: R_1^{(1)} + R_1^{(2)} \leq R_1^V, \\ & \mathrm{C}_5: P_1 + P_2 \leq P_{\max}^{\mathrm{VLC}}, \\ & \mathrm{C}_6: P_{\mathrm{RF}} \leq P_{\max}^{\mathrm{RF}}, \end{aligned} \tag{24}$$

where C_1 and C_2 denote the QoS requirement constraints for the cell-center and cell-edge users, respectively, C_3 is the Shannon capacity constraint of the RF sidelink, C_4 is the data rate constraint for the VLC channel between AP and U_1, and C_5, C_6 are the power consumption constraints. Note that the SIC constraint $R_{1\to2}^V \geq R_2^{\mathrm{thr}} - R_1^{(2)}$ is always fulfilled due to C_2 and the fact that $R_{1\to2}^V > R_2^V$ is observed when $h_1 > h_2$.

The optimization in (24) is a non-convex optimization problem. The reason of non-convexity is the existence of logarithmic functions with squared power terms in the expressions for the VLC achievable data rates in (9) and (10). Moreover, the objective function has a fractional form. To efficiently solve (24) in polynomial time, we need to transform it to an equivalent convex one. In line with this, we first introduce an auxiliary variable r_2 subject to:

$$R_2^{\mathrm{thr}} \leq r_2 \leq R_2^V + R_1^{(2)}. \tag{25}$$

This definition affects the objective function by removing from its expression the non-convex term R_2^V, thanks to its replacement by the new variable r_2. It also affects C_2 and introduces a new constraint, C_7. To this end, (24) becomes

$$\begin{aligned} \max_{P_1,P_2,P_{\mathrm{RF}},R_1^{(1)},R_1^{(2)},r_2} \quad & \frac{\alpha R_1^{(1)} + (1-\alpha)r_2}{\beta P_{\mathrm{LED}} + (1-\beta)P_{\mathrm{RF}}} \\ \text{s.t.} \quad & \mathrm{C}_1: R_1^{(1)} \geq R_1^{\mathrm{thr}}, \\ & \mathrm{C}_2: r_2 \geq R_2^{\mathrm{thr}}, \\ & \mathrm{C}_3: R_1^{(2)} \leq R_2^{\mathrm{RF}}, \\ & \mathrm{C}_4: R_1^{(1)} + R_1^{(2)} \leq R_1^V, \\ & \mathrm{C}_5: P_1 + P_2 \leq P_{\max}^{\mathrm{VLC}}, \\ & \mathrm{C}_6: P_{\mathrm{RF}} \leq P_{\max}^{\mathrm{RF}}, \\ & \mathrm{C}_7: r_2 - R_1^{(2)} \leq R_2^V. \end{aligned} \tag{26}$$

Due to the fractional form of the objective function, we utilize Dinkelbach's algorithm for fractional programming, which converges superlinearly [36]. This iterative algorithm introduces a parameter u, which corresponds to the original fraction, and solves an equivalent parametric program to find the maximum u. Specifically, considering the fractional program **max** $\{U(z) = F(z)/G(z)\}$, Dinkelbach's algorithm solves the following equivalent parametric program:

$$H(u) = \max\left\{F(z) - u_\lambda G(z)\right\}. \tag{27}$$

In iteration λ, $u_{\lambda+1}$ must be renewed, such that $u_{\lambda+1} = U(z_\lambda) = F(z_\lambda)/G(z_\lambda)$ until $u_{\lambda+1} < \epsilon$, where ϵ denotes the convergence accuracy. $H(u_\lambda)$ is continuous, convex and strictly decreasing in $\mathbb{R}$. Note that z^+ is optimal if and only

Algorithm 1: Dinkelbach's Algorithm

Initialization: Set the initial point $u_0 < u^+$, e.g., $u_0 = U(z_0) > 0$ for some z_0. Also, set iteration index $\lambda = 0$ and the convergence accuracy ϵ;
while $H(u_\lambda) > \epsilon$ (for a given ϵ) **do**
  Calculate an optimal solution z_i of $H(u_\lambda)$ s.t. C_1-C_7 in (28);
  Let $u_{\lambda+1} = U(z_\lambda)$;
  $\lambda \leftarrow \lambda + 1$;
end
Result: Optimal u^+, z^+

if it is optimal for $H(u_\lambda^+)$, where u_λ^+ is the only zero of H. Dinkelbach also noted that if F is concave and G is convex and positive, this algorithm leads to a convex program. In our case, $F = \alpha R_1^{(1)} + (1-\alpha) r_2$ and $G = \beta(P_1 + P_2) + (1-\beta) P_{\mathrm{RF}}$ are both affine, continuous and positive functions. Thus, (26) can be written as

$$\begin{aligned} \max_{z} \quad & F\left(R_1^{(1)}, r_2\right) - u_i G(P_1, P_2, P_{\mathrm{RF}}) \\ \text{s.t.} \quad & \mathrm{C}_1 : R_1^{(1)} \geq R_1^{\mathrm{thr}}, \\ & \mathrm{C}_2 : r_2 \geq R_2^{\mathrm{thr}}, \\ & \mathrm{C}_3 : R_1^{(2)} \leq R_2^{\mathrm{RF}}, \\ & \mathrm{C}_4 : R_1^{(1)} + R_1^{(2)} \leq R_1^{V}, \\ & \mathrm{C}_5 : P_1 + P_2 \leq P_{\max}^{\mathrm{VLC}}, \\ & \mathrm{C}_6 : P_{\mathrm{RF}} \leq P_{\max}^{\mathrm{RF}}, \\ & \mathrm{C}_7 : r_2 - R_1^{(2)} \leq R_2^{V}, \end{aligned} \tag{28}$$

where $z = [P_1, P_2, P_{\mathrm{RF}}, R_1^{(1)}, R_1^{(2)}, r_2]$ and u is fixed in each iteration. Dinkelbach's algorithm is presented in Algorithm 1, where the outputs z^+ and u^+ denote the optimal resource allocation vector and the maximized EE, respectively.

Next, we should deal with the non-convex constraints C_4 and C_7. For this, we apply the geometric programming transformations $P_1 = e^{p_1}$ and $P_2 = e^{p_2}$, which affects G, C_4, C_5, C_7 and z. It is possible to show that this transformation does not affect the convexity of G and C_5, but leads to a DC format for C_4 and C_7. As a result, unstable convexity issues of the last two aforementioned constraints can be overcome, and the problem can be solved in a tractable way. Thus, with the aid of (9), constraint C_4 can be rewritten as

$$2^{\left(R_1^{(1)} + R_1^{(2)} + \epsilon_\phi\right)/B_v} - 1 - v_1(p_1) \leq 0, \tag{29}$$

where $v_1(p_1) = c_1 e^{2p_1}$ and $c_1 = \frac{(\eta h_1)^2}{9\sigma^2(1+\epsilon_\mu)^2}$. Using (10) and performing similar algebraic manipulations, C_7 can be expressed as

$$\log\left(e^{2p_1} + c_2\right) + \frac{\log(2)}{B_v}\left(r_2 - R_1^{(2)} + \epsilon_\phi\right) - v_2(p_1, p_2), \tag{30}$$

where $v_2(p_1, p_2) = \log\left(e^{2p_1} + \frac{e^{2p_2}}{c_3} + c_2\right)$, $c_2 = 9\sigma^2/(\eta h_2)^2$ and $c_3 = (1 + \epsilon_\mu)^2$. Therefore, C_4 and C_7 are now DC functions.

To this end, we can use SCA procedure to approximate the non-convex terms in each iteration by using first-order Taylor series approximation, which has been proven to have linear convergence [37]. In [38], this method is considered as an inner approximation algorithm for programs with convex objective functions and a finite number of both convex and non-convex constraints. It is noted that the approximating functions must fulfill three properties for the algorithm's success, which are given by

$$g_{\mathrm{or}}(x) \leq g_{\mathrm{app}}(x; x^k), \tag{31}$$

$$g_{\mathrm{or}}(x^k) = g_{\mathrm{app}}(x^k; x^k), \tag{32}$$

$$\partial g_{\mathrm{or}}(x^k)/\partial x_j = \partial g_{\mathrm{app}}(x^k; x^k)/\partial x_j, \tag{33}$$

where g_{or} represents any differentiable function and g_{app} is any convex function that approximates g_{or}. Also, k is the iteration index for the SCA procedure. Moreover, first-order Taylor series expansion for a fixed point x^k can be written as

$$T_{\{1,2\}}(x) \approx v_{\{1,2\}}(x^k) + \nabla v_{\{1,2\}}(x^k)^T (x - x^k), \tag{34}$$

helping us to prove that (31)-(33) are valid. Then, replacing v_1 and v_2 with their closed-form expressions, we obtain

$$v_1(p_1) \approx T_1\left(p_1; p_1^k\right) = c_1 e^{2p_1^k}\left(1 + 2e^{2p_1} - 2e^{2p_1^k}\right) \tag{35}$$

and

$$\begin{aligned} v_2(p_1, p_2) \approx T_2\left(p_1, p_2; p_1^k, p_2^k\right) = v_2\left(p_1^k, p_2^k\right) \\ + \frac{\partial v_2\left(p_1^k, p_2^k\right)}{\partial p_1}\left(p_1 - p_1^k\right) + \frac{\partial v_2\left(p_1^k, p_2^k\right)}{\partial p_2}\left(p_2 - p_2^k\right), \end{aligned} \tag{36}$$

where

$$\frac{\partial v_2}{\partial p_1} = \frac{2e^{2p_1}}{e^{2p_1} + \frac{e^{2p_2}}{c_3} + c_2} \tag{37}$$

and

$$\frac{\partial v_2}{\partial p_2} = \frac{2e^{p_2}}{c_3(e^{2p_1} + \frac{e^{2p_2}}{c_3} + c_2)} \tag{38}$$

are the first order derivatives of v_2 with respect to p_1 and p_2, respectively. To this end, the considered optimization problem can be rewritten as

$$\begin{aligned} \max_{z} \quad & \alpha R_1^{(1)} + (1-\alpha) r_2 - u_\lambda\left(\beta(e^{p_1} + e^{p_2}) + (1-\beta) P_{\mathrm{RF}}\right) \\ \text{s.t.} \quad & \mathrm{C}_1 : R_1^{(1)} \geq R_1^{\mathrm{thr}}, \\ & \mathrm{C}_2 : r_2 \geq R_2^{\mathrm{thr}}, \\ & \mathrm{C}_3 : R_1^{(2)} \leq R_2^{\mathrm{RF}}, \\ & \mathrm{C}_4 : 2^{(R_1^{(1)} + R_1^{(2)} + \epsilon_\phi)/B_v} - 1 - T_1(p_1; p_1^k) \leq 0, \\ & \mathrm{C}_5 : e^{p_1} + e^{p_2} \leq P_{\max}^{\mathrm{VLC}}, \\ & \mathrm{C}_6 : P_{\mathrm{RF}} \leq P_{\max}^{\mathrm{RF}}, \\ & \mathrm{C}_7 : \log(e^{2p_1} + c_2) + \frac{\log(2)}{B_v}(r_2 - R_1^{(2)} + \epsilon_\phi) \\ & \qquad - T_2(p_1, p_2; p_1^k, p_2^k) \leq 0, \end{aligned} \tag{39}$$

which is a convex problem. As stated in [38], if (39) satisfies Slater's constraint qualification condition for convex programs, SCA stops at a Karush–Kuhn–Tucker (KKT) point of (28). Considering that (39) is convex, it can be easily proven than Slater's condition is satisfied. Thus, in each iteration, we obtain the global optimal values of z_λ^{k+1} until they converge. The SCA algorithm is presented in Algorithm 2.

The selection of a feasible initial point is an important issue for the success of the SCA procedure [39]. Our goal is either to obtain the initial z that fulfills both (29) and (30), or to show that our problem is infeasible and stop the procedure.

Algorithm 2: SCA Algorithm

Initialization: Set the initial point z_λ^0. Also, set iteration index $k=0$ and the convergence accuracy ϵ;
while $C_{\rm SCA} > \epsilon$ (for a given ϵ) **do**
  Calculate an optimal solution z_λ^{k+1} of (39);
  Let $C_{\rm SCA} = ||z_\lambda^k - z_\lambda^{k+1}||_2^2$;
  $k \leftarrow k+1$;
end
Result: Optimal $(z_\lambda^{k+1})^+$

For this purpose, we now formulate the power minimization problem of the VLC/RF system under consideration and study its feasibility. If the solution satisfies the constraints C_5 and C_6 of (24), we consider that the optimization problem is feasible and its solution can be used as initial point for the SCA procedure. The power minimization problem is formulated as

$$\begin{aligned} \min_{p_1,p_2,P_{\rm RF},R_1^{(1)},R_1^{(2)},r_2} \quad & \beta(e^{p_1}+e^{p_2})+(1-\beta)P_{\rm RF} \\ \text{s.t.} \quad & \mathrm{C}_1: R_1^{(1)}+R_1^{(2)} \le R_1^V, \\ & \mathrm{C}_2: r_2 - R_1^{(2)} \le R_2^V, \\ & \mathrm{C}_3: R_1^{(2)} \le R_2^{\rm RF}, \\ & \mathrm{C}_4: R_1^{(1)} \ge R_1^{\rm thr}, \\ & \mathrm{C}_5: r_2 \ge R_2^{\rm thr}. \end{aligned} \tag{40}$$

Using the coefficient $\theta \in [0,1]$, such that for the RF sidelink data rate verifies $R_1^{(2)} = \theta R_2^{\rm thr}$, with $e^{-\tilde{r}_1} = R_1^{(1)} + R_1^{(2)}$ and $e^{-\tilde{r}_2} \ge R_2^{\rm thr} - R_1^{(2)}$, (40) can be equivalently transformed into

$$\begin{aligned} \min_{p_1,p_2,P_{\rm RF},\tilde{r}_1,\tilde{r}_2,\theta} \quad & \beta(e^{p_1}+e^{p_2})+(1-\beta)P_{\rm RF} \\ \text{s.t.} \quad & \mathrm{C}_1: -2p_1 - \log(c_1) \\ & \qquad + \log(2^{(e^{\tilde{r}_1}+\epsilon_\phi)/B_v} - 1) \le 0, \\ & \mathrm{C}_2: \log(e^{2p_1}+c_2) - 2p_2 + \log(c_3) \\ & \qquad + \log(2^{(e^{\tilde{r}_2}+\epsilon_\phi)/B_v} - 1) \le 0, \\ & \mathrm{C}_3: \theta R_2^{\rm thr} \le R_2^{\rm RF}, \\ & \mathrm{C}_4: e^{-\tilde{r}_1} R_1^{\rm thr} + e^{-\tilde{r}_1}\theta R_2^{\rm thr} \le 1, \\ & \mathrm{C}_5: e^{-\tilde{r}_2}\left((1-\theta)R_2^{\rm thr}\right) \le 1, \\ & \mathrm{C}_6: 0 \le \theta \le 1. \end{aligned} \tag{41}$$

Proposition 1: Considering a fixed value of θ, (41) is a convex optimization problem.

Proof: The proof is provided in Appendix A. ■

Therefore, the most appropriate initial point is chosen from the value of θ and the corresponding solution of (41). To determine the value of θ, we perform a complete linear search in the interval $[0,1]$ with step j_θ, and solve (41) at each step. Due to its convex form, (41) can be efficiently solved with convex optimization methods, such as the interior-point method, and convergence can be reached in polynomial time.

After solving (41) and obtaining the optimal $z_\theta^* = [\tilde{r}_1^\theta, \tilde{r}_2^\theta, p_1^\theta, p_2^\theta, P_{\rm RF}^\theta]$ for all θ, we first obtain the combination $\theta^*, z_{\theta^*}^*$ which minimizes the objective function of (41). Next, we check if the power consumption constraints C_5 and C_6 in (39) are verified for $p_1^{\theta^*}$, $p_2^{\theta^*}$ and $P_{\rm RF}^{\theta^*}$. If they are not verified, we consider that the optimization problem is infeasible and stop the process. Otherwise, we obtain the initial feasible point $z_{\rm in} = \left[R_{1,\rm in}^{(1)}, R_{1,\rm in}^{(2)}, r_{2,\rm in}, p_{1,\rm in}, p_{2,\rm in}, P_{\rm RF,in}\right]$ as follows:

Algorithm 3: Utilized Algorithm

Data: Simulation parameters and $h_1, h_2, h_{\rm RF}, R_1^{\rm thr}, R_2^{\rm thr}$
Solve convex optimization problem (41) to obtain $z_{\theta^*}^*$;
if $e^{p_1^{\theta^*}} + e^{p_1^{\theta^*}} \le P_{\max}^{\rm VLC}$ **and** $P_{\rm RF}^{\theta^*} \le P_{\max}^{\rm RF}$ **then**
  Use (42) to obtain z_{in};
  Set $i=0$ and begin iterations of Algorithm 1;
  Set $k=0$ and begin iterations of Algorithm 2;
  Obtain optimal z^+
else
  Consider problem infeasible

$$\begin{aligned} R_{1,\rm in}^{(1)} &= e^{\tilde{r}_1^{\theta^*}} - \theta^* R_2^{\rm thr}, & R_{1,\rm in}^{(2)} &= \theta^* R_2^{\rm thr}, \\ r_{2,\rm in} &= e^{\tilde{r}_2^{\theta^*}} + \theta^* R_2^{\rm thr}, & p_{1,\rm in} &= p_1^{\theta^*}, \\ p_{2,\rm in} &= p_2^{\theta^*}, & P_{\rm RF,in} &= P_{\rm RF}^{\theta^*}. \end{aligned} \tag{42}$$

This algorithm is presented in Algorithm 3, which provides the optimal values for z^+. Regarding the computational complexity of the proposed algorithm, let $\mathcal{K}_1$ denote the maximum iterations of Dinkelbach's algorithm and $\mathcal{K}_2$ the maximum iterations of SCA procedure to verify the convergence condition. The worst case in terms of computational complexity is given by $\mathcal{O}(\mathcal{K}_1\mathcal{K}_2\mathcal{N}^3)$, where $\mathcal{N}$ is the number of optimization variables. Considering that a convex optimization is solved to determine the initial point of this procedure, the overall computational complexity becomes $\mathcal{O}(\mathcal{N}_{in}^3) + \mathcal{O}(\mathcal{K}_1\mathcal{K}_2\mathcal{N}^3)$, where $\mathcal{O}(\mathcal{N}^3)$ is the computational complexity of the interior-point method and $\mathcal{N}_{in}$ denotes the number of optimization variables of the initial point search procedure. Note that in case a different convex optimization method is utilized with known computational complexity $\mathcal{F}(\mathcal{N})$, the overall complexity of the proposed algorithm will become $\mathcal{F}(\mathcal{N}_{in}) + \mathcal{K}_1\mathcal{K}_2\mathcal{F}(\mathcal{N})$.

Special Case: Non-aggregated VLC/RF Combining

As explained before, the special case of VLC/RF non-aggregated combining reduces naturally to a simpler optimization problem. More specifically, when plugging (25) into (20),

$$R_2^{\rm thr} \le r_2 \le q R_2^{\rm RF} + (1-q) R_2^V \tag{43}$$

results, which falls into the category of mixed integer nonlinear programming. Since the integer variable q of the optimization problem can only take two distinct values, the problem can be simplified by first performing a search on q, then solving the resulting problem with the rest of the optimization variables, and finally choosing the optimal value of q. To further elaborate on this, the optimization problems that result for each possible value of q are now presented.

TABLE I
SIMULATION PARAMETERS OF THE VLC/RF NETWORK

Parameter	Value	Parameter	Value
$P_{\max}^{\mathrm{VLC}}$	750 mW	σ^2	$5\times10^{-22}\mathrm{A}^2$
$P_{\max}^{\mathrm{RF}}$	200 mW	σ_R^2	$4.002\times10^{-14}\mathrm{W}$
R_0	1.5 m	$T(\psi_i)$	1
R_v	3 m	Ψ_{FoV}	$\pi/3$
L	2.15 m	$\Phi_{1/2}$	$\pi/3$
ν	1.5	A_r	1 cm^2
ζ	2	η	0.5 A/W
K_r	2.41	Ω	1

For $q=0$, optimization problem (39) is transformed into

$$\begin{aligned}\max_{z}\quad & \alpha R_1^{(1)}+(1-\alpha)r_2-u_\lambda\big(\beta(e^{p_1}+e^{p_2})+(1-\beta)P_{\mathrm{RF}}\big)\\ \text{s.t.}\quad & \mathrm{C}_1: R_1^{(1)}\geq R_1^{\mathrm{thr}},\\ & \mathrm{C}_2: r_2\geq R_2^{\mathrm{thr}},\\ & \mathrm{C}_3: 2^{(R_1^{(1)}+\epsilon_\phi)/B_v}-1-T_1(p_1;p_1^k)\leq 0,\\ & \mathrm{C}_4: e^{p_1}+e^{p_2}\leq P_{\max}^{\mathrm{VLC}},\\ & \mathrm{C}_5: \log(e^{2p_1}+c_2)+\frac{\log(2)}{B_v}(r_2+\epsilon_\phi)\\ & \quad -T_2(p_1,p_2;p_1^k,p_2^k)\leq 0.\end{aligned} \tag{44}$$

Similarly, the consequent problem for $q=1$ becomes

$$\begin{aligned}\max_{z}\quad & \alpha R_1^{(1)}+(1-\alpha)r_2-u_\lambda\big(\beta(e^{p_1}+e^{p_2})+(1-\beta)P_{\mathrm{RF}}\big)\\ \text{s.t.}\quad & \mathrm{C}_1: R_1^{(1)}\geq R_1^{\mathrm{thr}},\\ & \mathrm{C}_2: r_2\geq R_2^{\mathrm{thr}},\\ & \mathrm{C}_3: 2^{(R_1^{(1)}+\epsilon_\phi)/B_v}-1-T_1(p_1;p_1^k)\leq 0,\\ & \mathrm{C}_4: e^{p_1}+e^{p_2}\leq P_{\max}^{\mathrm{VLC}},\\ & \mathrm{C}_5: P_{\mathrm{RF}}\leq P_{\max}^{\mathrm{RF}},\\ & \mathrm{C}_6: \log(e^{2p_1}+c_2)+\frac{\log(2)}{B_v}(r_2+\epsilon_\phi)\\ & \quad -T_2(p_1,p_2;p_1^k,p_2^k)\leq 0,\\ & \mathrm{C}_7: \log\left(e^{2p_1}+\frac{9\sigma^2}{(\eta h_1)^2}\right)-2p_2\\ & \quad +\log\left((1+\epsilon_\mu)^2(2^{\frac{R_2^{\mathrm{thr}}+\epsilon_\phi}{B_v}}-1)\right)\leq 0.\end{aligned} \tag{45}$$

Problems (44) and (45) are both convex and can be solved with conventional convex optimization methods. Note that, in both special cases, Algorithm 3 is utilized, but the constraints of the resulting SCA procedure differ from the constraints of the general case.

V. SIMULATION RESULTS AND DISCUSSION

In this section, Monte Carlo simulation results are presented for the proposed algorithm for 10^4 snapshots in which the positions of the users change. The convergence accuracy ϵ for the two iterative algorithms are set equal to 10^{-6}, while the selected step size is $j_\theta=10^{-2}$. For the sake of simplicity, unless otherwise stated, we consider that users have common QoS requirements, which we denote as $R^{\mathrm{thr}}=R_1^{\mathrm{thr}}=R_2^{\mathrm{thr}}$. The utilized parameters for the simulation results are presented in Table I. The bandwidth of the VLC subsystem is set $B_v=4\,B_R$.

The performance of the proposed VLC/RF aggregated approach is compared with a conventional network setup, i.e., the non-aggregated VLC/RF approach considered in [1]. Since the superiority of NOMA has been established over standard orthogonal schemes, especially for two-user configurations, these cases can be considered as a benchmark scheme. As such, Fig. 2 presents the comparison between the proposed protocol and the benchmark, namely pure VLC, where the RF sidelink is not used, and the non-aggregated hybrid VLC/RF for the same fixed values of α and β. Based on this figure, the proposed protocol outperforms the two VLC/RF non-aggregated modes presented in [1]. For low QoS requirements, the proposed VLC/RF system exhibits better performance as $x_1^{(2)}$ is decoded by cell-center user U_1 without interference. For high target data rates, the performance of the proposed protocol converges to the one of the VLC-NOMA scheme presented in [1].

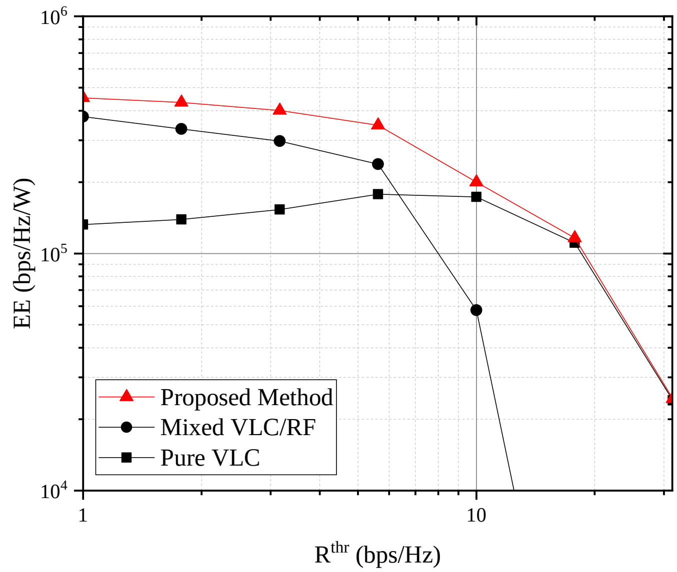

Fig. 2. EE versus R^{thr} comparison between non-aggregated special cases and aggregated approach for $\alpha=\beta=0.5$.

In Fig. 3, the EE is plotted versus the R^{thr} for different fixed values of the throughput tuning weight α. It is noted that the different values of α highlight whether priority is given to one user over the other in terms of the achievable data rate. Setting $\beta=0.5$ means that both power sources are equally accountable for the energy consumption of the aggregated VLC/RF network. It can be observed that, while α increases, higher EE can be achieved for low QoS requirements, however the value of α does not have any impact when higher data rates must be achieved. When priority can be given, it is easier for cell-center user U_1 to achieve a higher data rate with a lower energy consumption when compared to cell-edge user U_2. In the scenario that gives priority to U_2 (i.e., when $\alpha<0.5$), a lower EE is inevitable due to the more demanding VLC link budget because of a longer distance from the VLC-AP when compared to user U_1, or due to the use of the RF sidelink to forward part of the information intended to user U_2.

In Fig. 4, we set $\alpha=0.5$, so that both users have the same priority and investigate the impact of β. To provide further insights, low values of β (i.e., $\beta<0.5$) represent scenarios,

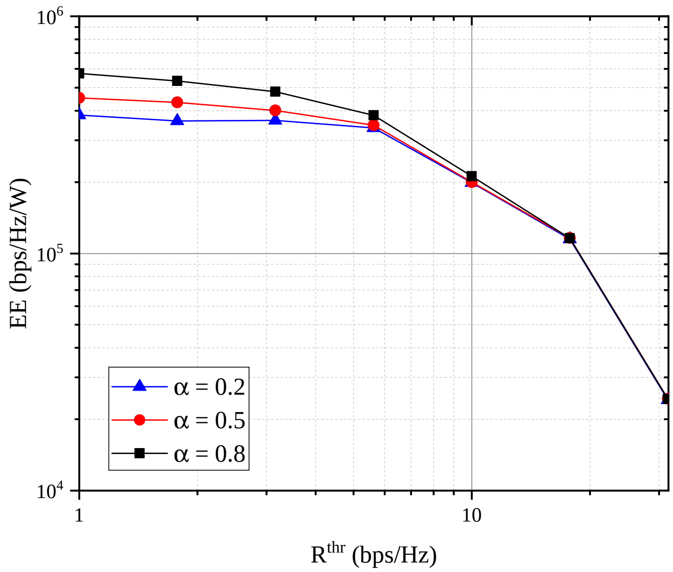

Fig. 3. EE of the aggregated network versus R^{thr} for different α values.

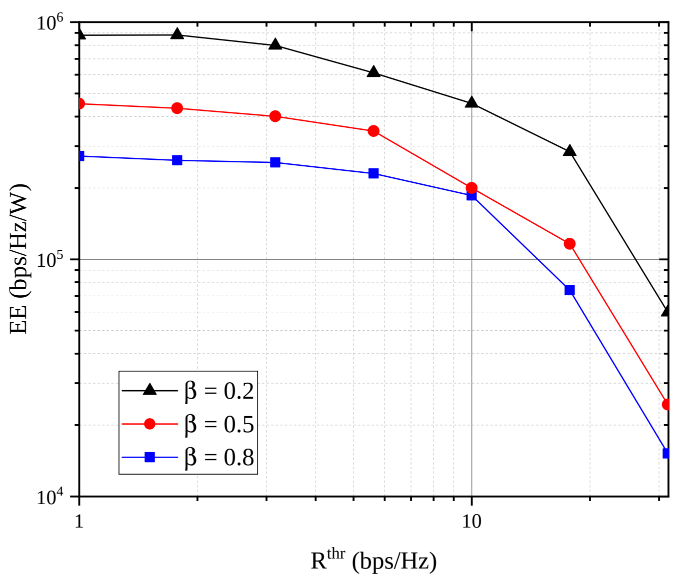

Fig. 4. EE of the aggregated network versus R^{thr} for different β values.

where the LED is also used for illumination and, thus, it is not necessary to focus on its power consumption. It can be observed that this scenario is the most energy efficient, regardless of the QoS requirements. On the other hand, when the indoor illumination is not needed, β can be set higher than 0.5, to highlight the cost of VLC-AP. As expected, this turns out to be the least energy efficient scenario.

In Fig. 5, we set $\alpha = \beta = 0.5$ and we investigate the pure EE, without emphasizing either on achievable rate or on energy consumption. In this figure, the impact of higher QoS requirement of the cell-center user U_1 is illustrated. When U_1 requires higher data rate, the overall network becomes less energy efficient even for low target rate. Additionally, since the power consumption increases and tends to exceed permissible limits, i.e., $P_{\max}^{\text{VLC}}$ and $P_{\max}^{\text{RF}}$, our network cannot

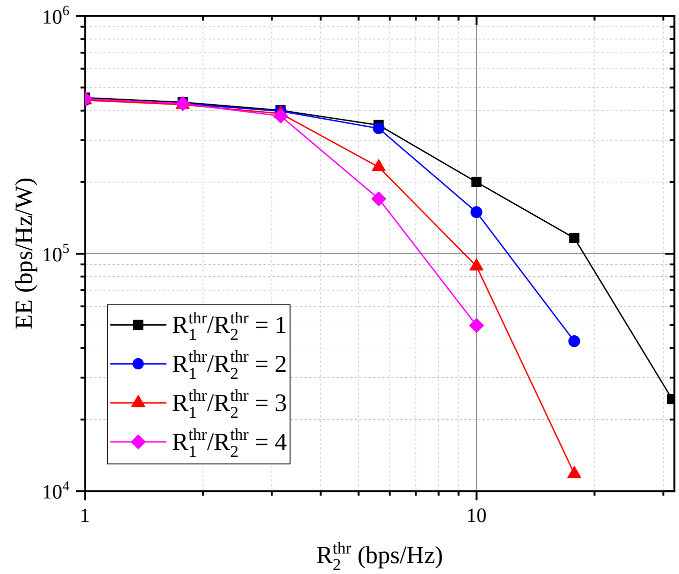

Fig. 5. EE versus R^{thr} for different QoS requirements and weight settings $\alpha = \beta = 0.5$.

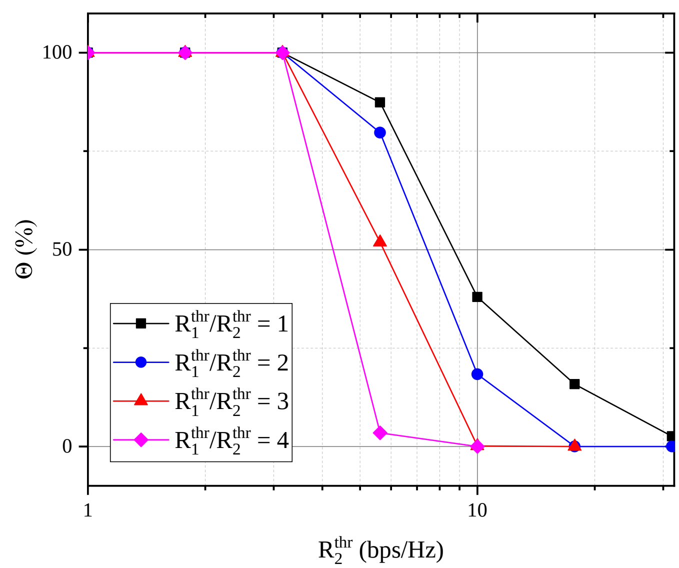

Fig. 6. RF link usage versus R_2^{thr} for weight settings $\alpha = \beta = 0.5$.

operate efficiently in the region above 10 bps/Hz.

To derive further insight to the proposed network's operation, we denote as RF link's usage $\Theta = \frac{R_1^{(2)}}{R_1^{(2)}+R_2^{V}}$ the ratio between the rate of decoded and retransmitted data by U_1 and the total achievable rate of U_2. In Fig. 6, Θ is plotted versus R_2^{thr} with $\alpha = \beta = 0.5$. It can be observed that for low target rates the RF link is exclusively advantageous, while as the QoS requirements increase, VLC plays a dominant role in providing service to U_2 that has a weaker received signal.

Following that, we define $\gamma = \frac{L_{\text{RF}}|h_{\text{RF}}|^2 P_{\text{RF}}}{\sigma_{\text{R}}^2}$ to investigate its impact on both EE and Θ. In Fig. 7 the unweighted EE is studied by setting $\alpha = \beta = 0.5$, as illustrated in Fig. 6, and $R^{\text{thr}} = 10$ bps/Hz is set. Fig. 7 highlights that, while γ goes higher, EE increases by 2×10^4 bps/Hz/W, which

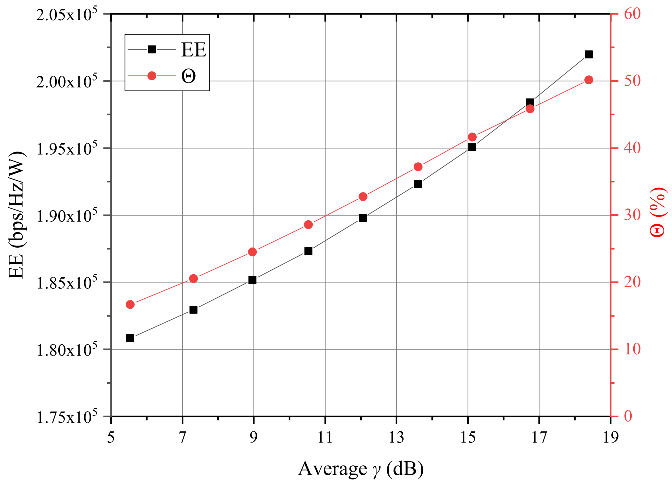

Fig. 7. EE and Θ of the aggregated network versus average γ for settings $\alpha = \beta = 0.5$ and $R^{\text{thr}} = 10$ bps/Hz.

means that a high RF channel gain contributes significantly in the improvement of overall system's performance. Finally, the red curve in 7 illustrates the RF link's usage ratio Θ which increases as the RF channel gain improves, in a similar manner as the EE.

VI. Conclusions

In this work, we investigated a cross-band aggregated VLC/RF network with an RF relay link from a cell-center user to a cell-edge one, aiming to improve the latter's performance with the assumption that the cell-edge user receives its message from both VLC and RF links in an aggregated manner. To maximize the EE of the network, a resource allocation optimization problem was proposed, which was subsequently solved by combining Dinkelbach's and SCA algorithms. The presented numerical results validated proposed analysis and provided further insight into the impact of the involved parameters in the aggregated system's performance. Future research will encompass the multi-cell extension of the network, investigating interference management solutions, as well as user scheduling methods.

Appendix A
Proof of Proposition 1

In (40), we let $r_1 = R_1^{(1)} + R_1^{(2)}$ to denote the sum-rate decoded by U_1 which cannot exceed R_1^V and $\bar{r}_2 = r_2 - R_1^{(2)}$ the rate that U_2 decodes $x_2^{(2)}$, which cannot exceed R_2^V. It should be highlighted that r_1 must be greater than $R_1^{\text{thr}} + R_1^{(2)}$. Similarly, $\bar{r}_2$ should satisfy the QoS requirement for cell-edge's user VLC channel, so $\bar{r}_2 \geq R_2^{\text{thr}} - R_1^{(2)} = (1-\theta)R_2^{\text{thr}}$. Therefore, (40) can be written as

$$\begin{aligned} \min_{p_1,p_2,P_{\text{RF}},r_1,\bar{r}_2,\theta} \quad & \beta(e^{p_1} + e^{p_2}) + (1-\beta)P_{\text{RF}} \\ \textbf{s.t.} \quad & \mathrm{C}_1 : r_1 \leq R_1^V, \\ & \mathrm{C}_2 : \bar{r}_2 \leq R_2^V, \\ & \mathrm{C}_3 : \theta R_2^{\text{thr}} \leq R_2^{\text{RF}}, \\ & \mathrm{C}_4 : r_1 \geq R_1^{\text{thr}} + \theta R_2^{\text{thr}}, \\ & \mathrm{C}_5 : \bar{r}_2 \geq (1-\theta) R_2^{\text{thr}}, \\ & \mathrm{C}_6 : 0 \leq \theta \leq 1. \end{aligned} \tag{46}$$

Considering a fixed θ, employing the geometric programming transformations $e^{\tilde{r}_1} = r_1$ and $e^{\tilde{r}_2} = \bar{r}_2$ and after some algebraic manipulations, (46) is transformed into a convex optimization problem as follows

$$\begin{aligned} \min_{p_1,p_2,P_{\text{RF}},\tilde{r}_1,\tilde{r}_2} \quad & \beta(e^{p_1} + e^{p_2}) + (1-\beta)P_{\text{RF}} \\ \textbf{s.t.} \quad & \mathrm{C}_1 : -2p_1 - \log(c_1) \\ & \qquad + \log(2^{(e^{\tilde{r}_1}+\epsilon_\phi)/B_v} - 1) \leq 0, \\ & \mathrm{C}_2 : \log(e^{2p_1} + c_2) - 2p_2 + \log(c_3) \\ & \qquad + \log(2^{(e^{\tilde{r}_2}+\epsilon_\phi)/B_v} - 1) \leq 0, \\ & \mathrm{C}_3 : \theta R_2^{\text{thr}} \leq R_2^{\text{RF}}, \\ & \mathrm{C}_4 : e^{\tilde{r}_1} \geq R_1^{\text{thr}} + \theta R_2^{\text{thr}}, \\ & \mathrm{C}_5 : e^{\tilde{r}_2} \geq (1-\theta) R_2^{\text{thr}}. \end{aligned} \tag{47}$$

To prove the convexity, first we rewrite C_4 and C_5 in (47), respectively, as

$$\mathrm{C}_4 : R_1^{\text{thr}} e^{-\tilde{r}_1} + \theta R_2^{\text{thr}} e^{-\tilde{r}_1} \leq 1 \tag{48}$$

$$\mathrm{C}_5 : (1-\theta) R_2^{\text{thr}} e^{-\tilde{r}_2} \leq 1. \tag{49}$$

It can be observed that C_4 and C_5 are convex, since θ and $(1-\theta)$ are positive. Moreover, C_1 and C_2 consist of linear and convex terms, i.e., $\log(e^{2p_1} + c_2)$ is convex as a log-sum-exp term and $\log(2^{(e^{\tilde{r}_1}+\epsilon_\phi)/B_v} - 1)$ and $\log(2^{(e^{\tilde{r}_2}+\epsilon_\phi)/B_v} - 1)$ are convex, because their second derivative with respect to $\tilde{r}_1$ and $\tilde{r}_2$, respectively, is positive, as presented below. The derivative is calculated as

$$\frac{\frac{\log(2)}{B_v} 2^{\frac{e^{\tilde{r}_{1,2}}+\epsilon_\phi}{B_v}} e^{\tilde{r}_{1,2}} \left(2^{\frac{e^{\tilde{r}_{1,2}}+\epsilon_\phi}{B_v}} - e^{\tilde{r}_{1,2}} \frac{\log(2)}{B_v} - 1 \right)}{\left(2^{\frac{e^{\tilde{r}_{1,2}}+\epsilon_\phi}{B_v}} - 1 \right)^2}. \tag{50}$$

Considering that $\xi = 2^{\frac{e^{\tilde{r}_{1,2}}+\epsilon_\phi}{B_v}} - e^{\tilde{r}_{1,2}} \frac{\log(2)}{B_v} - 1$ is an increasing function with respect to $\tilde{r}_{1,2}$ and when $\tilde{r}_{1,2} \to -\infty$, $\xi \to 2^{\frac{\epsilon_\phi}{B_v}} - 1 > 0$, because $\frac{\epsilon_\phi}{B_v} > 0$. Also, C_6 is affine, C_3 is convex due to the concavity of R_2^{RF}. Finally, the objective function is also convex as sum of exponentials, so the proof is completed.

References

[1] K. G. Rallis, V. K. Papanikolaou, P. D. Diamantoulakis, M.-A. Khalighi, and G. K. Karagiannidis, "Energy Efficiency Maximization in Cooperative Hybrid VLC/RF Networks with NOMA," in *Proc. 17th International Symposium on Wireless Communication Systems (ISWCS)*, Berlin, Germany, 2021, pp. 1–6.

[2] Ericsson, "Ericsson mobility report," Ericsson SE-164 80 Stockholm, Sweden, Telephone +46 10 719 0000, www.ericsson.com, EAB-21:005137 Uen, June 2021. [Online]. Available: https://www.ericsson.com/4a03c2/assets/local/reports-papers/mobility-report/documents/2021/june-2021-ericsson-mobility-report.pdf

[3] Cisco, "Cisco annual internet report (2018–2023)," C11-741490-01 03/20, 2020. [Online]. Available: https://www.cisco.com/c/en/us/solutions/collateral/executive-perspectives/annual-internet-report/white-paper-c11-741490.pdf

[4] V. K. Papanikolaou, P. D. Diamantoulakis, and G. K. Karagiannidis, *Hybrid Lightwave/RF Connectivity for 6G Wireless Networks*. Cham: Springer International Publishing, 2021, pp. 169–186. [Online]. Available: https://doi.org/10.1007/978-3-030-72777-2_9

[5] B. Genovés Guzmán, A. Dowhuszko, V. Gil Jiménez, and A. Pérez-Neira, "Cooperative transmission scheme to address random orientation and blockage events in VLC systems," in *Proc. Int. Symp. Wireless Commun. Systems*, Aug. 2019, pp. 351–355.

[6] M. Uysal, C. Capsoni, Z. Ghassemlooy, A. Boucouvalas, and E. Udvary, *Optical Wireless Communications: An Emerging Technology*. Springer, 2016.

[7] M. Z. Chowdhury, M. K. Hasan, M. Shahjalal, M. T. Hossan, and Y. M. Jang, "Optical Wireless Hybrid Networks: Trends, Opportunities, Challenges, and Research Directions," *Commun. Surveys Tuts.*, vol. 22, no. 2, pp. 930–966, 2020.

[8] H. Abuella, M. Elamassie, M. Uysal, Z. Xu, E. Serpedin, K. A. Qaraqe, and S. Ekin, "Hybrid RF/VLC Systems: A Comprehensive Survey on Network Topologies, Performance Analyses, Applications, and Future Directions," *IEEE Access*, pp. 1–1, 2021.

[9] D. Bozanis, V. K. Papanikolaou, A. A. Dowhuszko, K. G. Rallis, P. D. Diamantoulakis, J. Hämäläinen, and G. K. Karagiannidis, "Optimal Aggregation of RF and VLC Bands for Beyond 5G Mobile Services," in *18th International Conference on Wireless and Mobile Computing, Networking and Communications*, Thessaloniki, Greece, Oct. 2022, pp. 75–80.

[10] H. Sadat, M. Abaza, A. Mansour, and A. Alfalou, "A Survey of NOMA for VLC Systems: Research Challenges and Future Trends," *Sensors*, vol. 22, no. 4, 2022.

[11] L. Yin, W. O. Popoola, X. Wu, and H. Haas, "Performance Evaluation of Non-Orthogonal Multiple Access in Visible Light Communication," *IEEE Trans. Commun.*, vol. 64, no. 12, pp. 5162–5175, Dec. 2016.

[12] Z. Yang, W. Xu, and Y. Li, "Fair Non-Orthogonal Multiple Access for Visible Light Communication Downlinks," *IEEE Wireless Commun. Lett.*, vol. 6, no. 1, pp. 66–69, Feb. 2017.

[13] L. Zhang, Z. Wang, Y. Cai, R. Xie, J. Ma, H. Y. Fu, and Y. Dong, "Large-Coverage White-Light Controller Combining Adaptive QoS-Enhanced mQAM-NOMA for High-Speed Visible Light Communication," *J. Lightw. Technol.*, pp. 1–1, 2021.

[14] S. Aboagye, A. Ibrahim, T. M. N. Ngatched, and O. A. Dobre, "VLC in Future Heterogeneous Networks: Energy– and Spectral–Efficiency Optimization," in *Proc. IEEE International Conference on Communications (ICC)*, 2020, pp. 1–7.

[15] A. Khreishah, S. Shao, A. Gharaibeh, M. Ayyash, H. Elgala, and N. Ansari, "A Hybrid RF-VLC System for Energy Efficient Wireless Access," *IEEE Trans. Green Commun. Netw.*, vol. 2, no. 4, pp. 932–944, Dec. 2018.

[16] V. K. Papanikolaou, P. D. Diamantoulakis, P. C. Sofotasios, S. Muhaidat, and G. K. Karagiannidis, "On Optimal Resource Allocation for Hybrid VLC/RF Networks With Common Backhaul," *IEEE Trans. Cogn. Commun. Netw.*, vol. 6, no. 1, pp. 352–365, Mar. 2020.

[17] J. Kong, M. Ismail, E. Serpedin, and K. A. Qaraqe, "Energy Efficient Optimization of Base Station Intensities for Hybrid RF/VLC Networks," *IEEE Trans. Wireless Commun.*, vol. 18, no. 8, pp. 4171–4183, 2019.

[18] Y. Guo, K. Xiong, Y. Lu, D. Wang, P. Fan, and K. B. Letaief, "Achievable Information Rate in Hybrid VLC-RF Networks With Lighting Energy Harvesting," *IEEE Trans. Commun.*, vol. 69, no. 10, pp. 6852–6864, 2021.

[19] Y. Xiao, P. D. Diamantoulakis, Z. Fang, L. Hao, Z. Ma, and G. K. Karagiannidis, "Cooperative Hybrid VLC/RF Systems With SLIPT," *IEEE Trans. Commun.*, vol. 69, no. 4, pp. 2532–2545, 2021.

[20] S. Shao, A. Khreishah, M. Ayyash, M. B. Rahaim, H. Elgala, V. Jungnickel, D. Schulz, T. D. Little, J. Hilt, and R. Freund, "Design and analysis of a visible-light-communication enhanced wifi system," *IEEE J. Opt. Commun. Netw.*, vol. 7, no. 10, pp. 960–973, 2015.

[21] M. Ayyash, H. Elgala, A. Khreishah, V. Jungnickel, T. Little, S. Shao, M. Rahaim, D. Schulz, J. Hilt, and R. Freund, "Coexistence of WiFi and LiFi toward 5G: concepts, opportunities, and challenges," *IEEE Commun. Mag.*, vol. 54, no. 2, pp. 64–71, 2016.

[22] S. Aboagye, A. Ibrahim, T. M. N. Ngatched, A. R. Ndjiongue, and O. A. Dobre, "Design of Energy Efficient Hybrid VLC/RF/PLC Communication System for Indoor Networks," *IEEE Wireless Commun. Lett.*, vol. 9, no. 2, pp. 143–147, Feb. 2020.

[23] S. Aboagye, T. M. N. Ngatched, O. A. Dobre, and H. Vincent Poor, "Energy-Efficient Resource Allocation for Aggregated RF/VLC Systems," *IEEE Trans. Wireless Commun.*, pp. 1–1, Feb. 2023.

[24] K. Küçük, D. Msongaleli, O. Akbulut, A. Kavak, and C. Bayılmış, "Self-adaptive Medium Access Control protocol for Aggregated VLC–RF Wireless Networks," *Optics Communications*, vol. 488, p. 126837, 2021.

[25] F. Wang, F. Yang, C. Pan, J. Song, and Z. Han, "Hybrid VLC-RF Systems with Multi-users for Achievable Rate and Energy Efficiency Maximization," *IEEE Trans. Wireless Commun.*, pp. 1–1, Jan. 2023.

[26] A. Zubow, P. Gawowicz, C. Brunn, K. L. Bober, V. Jungnickel, K. Habel, and F. Dressler, "Hybrid-Fidelity: Utilizing IEEE 802.11 MIMO for Practical Aggregation of LiFi and WiFi," *IEEE Trans. Mob. Comput.*, pp. 1–1, Mar. 2022.

[27] V. K. Papanikolaou, P. D. Diamantoulakis, and G. K. Karagiannidis, "User Grouping for Hybrid VLC/RF Networks With NOMA: A Coalitional Game Approach," *IEEE Access*, vol. 7, pp. 103 299–103 309, Jul. 2019.

[28] A. al Hammadi, S. Muhaidat, P. C. Sofotasios, and M. al Qutayri, "A Robust and Energy Efficient NOMA-Enabled Hybrid VLC/RF Wireless Network," in *IEEE Wireless Communications and Networking Conference (WCNC)*, 2019, pp. 1–6.

[29] Y. Xiao, P. D. Diamantoulakis, Z. Fang, Z. Ma, L. Hao, and G. K. Karagiannidis, "Hybrid Lightwave/RF Cooperative NOMA Networks," *IEEE Trans. Wireless Commun.*, vol. 19, no. 2, pp. 1154–1166, Feb. 2020.

[30] M. Obeed, H. Dahrouj, A. M. Salhab, S. A. Zummo, and M.-S. Alouini, "User Pairing, Link Selection, and Power Allocation for Cooperative NOMA Hybrid VLC/RF Systems," *IEEE Trans. Wireless Commun.*, vol. 20, no. 3, pp. 1785–1800, Mar. 2021.

[31] M. Obeed, H. Dahrouj, A. M. Salhab, A. Chaaban, S. A. Zummo, and M.-S. Alouini, "Power Allocation and Link Selection for Multicell Cooperative NOMA Hybrid VLC/RF Systems," *IEEE Commun. Lett.*, vol. 25, no. 2, pp. 560–564, Feb. 2021.

[32] R. Raj and A. Dixit, "Outage Analysis and Reliability Enhancement of Hybrid VLC-RF Networks Using Cooperative Non-Orthogonal Multiple Access," *IEEE Trans. Netw. Service Manag.*, pp. 1–1, 2021.

[33] A. Chaaban, Z. Rezki, and M.-S. Alouini, "On the Capacity of the Intensity-Modulation Direct-Detection Optical Broadcast Channel," *IEEE Trans. Wireless Commun.*, vol. 15, no. 5, pp. 3114–3130, Jan. 2016.

[34] D. A. Basnayaka and H. Haas, "Design and Analysis of a Hybrid Radio Frequency and Visible Light Communication System," *IEEE Trans. Commun.*, vol. 65, no. 10, pp. 4334–4347, Oct. 2017.

[35] S. Ma, F. Zhang, H. Li, F. Zhou, M.-S. Alouini, and S. Li, "Aggregated VLC-RF Systems: Achievable Rates, Optimal Power Allocation, and Energy Efficiency," *IEEE Trans. Wireless Commun.*, vol. 19, no. 11, pp. 7265–7278, Jul. 2020.

[36] W. Dinkelbach, "On Nonlinear Fractional Programming," *Management Science*, vol. 13, no. 7, pp. 492–498, Mar. 1967.

[37] L. T. H. An and P. D. Tao, "The DC (difference of convex functions) programming and DCA revisited with DC models of real world nonconvex optimization problems," *Annals of operations research*, vol. 133, pp. 23–46, 2005.

[38] B. R. Marks and G. P. Wright, "Technical note—a general inner approximation algorithm for nonconvex mathematical programs," *Operations Research*, vol. 26, no. 4, pp. 681–683, aug 1978. [Online]. Available: https://doi.org/10.1287%2Fopre.26.4.681

[39] A. M. Abdelhady, O. Amin, A. Chaaban, B. Shihada, and M.-S. Alouini, "Downlink Resource Allocation for Dynamic TDMA-Based VLC Systems," *IEEE Trans. Wireless Commun.*, vol. 18, no. 1, pp. 108–120, Oct. 2019.

Konstantinos G. Rallis (Graduate Student Member, IEEE) received the Diploma from the Department of Electrical and Computer Engineering (ECE), Aristotle University of Thessaloniki (AUTH), Greece, in 2021 where he is currently pursuing his PhD with the Department of Electrical and Computer Engineering. He is a member of the Wireless and Communications and Information Processing (WCIP) group. His research interests include optical wireless communications, hybrid optical and RF networks, multiple access schemes, resource allocation, optimization theory and machine learning applications to wireless communications.

Vasilis K. Papanikolaou (Member, IEEE) received the Diploma (5 years) and PhD degrees in Electrical and Computer Engineering from the Aristotle University of Thessaloniki, Greece, in 2018 and 2023, respectively, where he was a member of the Wireless and Communications and Information Processing (WCIP) group. He is currently a Humboldt Post-Doctoral Research Fellow with the Institute for Digital Communications, Friedrich-Alexander-University Erlangen-Nurnberg (FAU), Erlangen, Germany. He was a Visiting Research Assistant with Lancaster University, UK, with Khalifa University, Abu Dhabi, UAE, and with the Northumbria University, Newcastle-upon-Tyne, UK. His major research interests include optical wireless communications, wireless power transfer, multiple access schemes, and optimization theory. He was an Exemplary Reviewer of the IEEE Wireless Communications Letters in 2019, 2020, and 2022 and of the IEEE Open Journal of the Communications Society in 2021 (top 3% of reviewers).

Panagiotis D. Diamantoulakis (Senior Member, IEEE) received the Diploma (five years) and PhD from the Department of Electrical and Computer Engineering (ECE), Aristotle University of Thessaloniki (AUTH), Greece, in 2012 and 2017, respectively. Since 2017, he works as a Post-doctoral Fellow in Wireless Communications and Information Processing (WCIP) group at AUTH and since 2021, he is a visiting Assistant Professor in the Key Lab of Information Coding and Transmission at Southwest Jiaotong University (SWJTU), China. His research interests include optimization theory and applications in wireless networks and smart grids, game theory, and optical wireless communications. He serves as an Editor for IEEE Wireless Communications Letters, IEEE Open Journal of the Communications Society, Physical Communications (Elsevier), and Frontiers in Communications and Networks.

Sotiris A. Tegos (Member, IEEE) received the Diploma (five years) and the PhD degree from the Department of Electrical and Computer Engineering, Aristotle University of Thessaloniki, Thessaloniki, Greece, in 2017 and 2022, respectively. He works as a Post-doctoral Fellow in the Wireless Communications and Information Processing (WCIP) group. In 2018, he was a Visitor Researcher with the Department of Electrical and Computer Engineering, Khalifa University, Abu Dhabi, United Arab Emirates. His research interests include wireless power transfer, optical wireless communications, and multiple access in wireless communications. He was an Exemplary Reviewer in IEEE Wireless Communications Letters for 2019 and 2022 (top 3% of reviewers).

Alexis A. Dowhuszko (Senior Member, IEEE) received the Telecommunications Engineer degree from Blas Pascal University, Córdoba, Argentina, in 2002, and the Ph.D. degree in engineering sciences from the Universidad Nacional de Córdoba, Córdoba, Argentina, in 2010. From 2010 to 2015, he was a Postdoctoral Researcher with the Department of Communications and Networking, Aalto University, Helsinki, Finland. In 2016, he moved to Spain to take a Senior Researcher position with the Centre Tecnològic de Telecomunicacions de Catalunya, Barcelona, Spain. In August 2020, he returned to Finland and joined Aalto University, as a Research Fellow. He has authored or coauthored more than 25 journal articles, 60 conference papers, one book chapter, and five patent applications.

Ali Khalighi (Senior Member, IEEE) is Associate Professor with École Centrale Méditérranée, Marseille, France, and head of Optical Communications for IoT group at the Fresnel Institute research lab. He is currently serving as Action Chair for the COST Action CA19111 NEWFOCUS, and also served as Project Coordinator for the H2020 ITN MSCA VisIoN project. He was the co-editer of the book "Visible Light Communications: Theory and Applications" (CRC Press, 2017) and the co-recipient of the 2019 Best Survey Paper Award of the IEEE Communications Society. He is also serving as Editor-at-Large for the IEEE Transactions on Communications. His main research interests include signal processing for wireless communication systems with an emphasis on free-space, underwater, and indoor visible-light optical communications.

George K. Karagiannidis (Fellow, IEEE) is currently Professor in the Electrical and Computer Engineering Dept. of Aristotle University of Thessaloniki, Greece and Head of Wireless Communications and Information Processing (WCIP) group. He is also Faculty Fellow in the Cyber Security Systems and Applied AI Research Center, Lebanese American University. His research interests are in the areas of Wireless Communications Systems and Networks, Signal processing, Optical Wireless Communications, Wireless Power Transfer and Applications and Communications and Signal Processing for Biomedical Engineering.

Prof. Karagiannidis was in the past Editor in several IEEE journals and from 2012 to 2015 he was the Editor-in Chief of IEEE Communications Letters. From September 2018 to June 2022 he served as Associate Editor-in Chief of IEEE Open Journal of Communications Society. Currently, he is in the Steering Committee of IEEE Transactions on Cognitive Communications and Networks.

Recently, he received two prestigious awards: The 2021 IEEE Communications Society Radio Communications (RCC) Committee Technical Recognition Award, for his Outstanding Contributions to Wireless Systems and the 2018 Signal Processing and Communications Electronics (SPCE) Technical Recognition Award of the IEEE ComSoc for his Outstanding Technical Contributions to Signal Processing for Communications.

Prof. Karagiannidis is one of the highly-cited authors across all areas of Electrical Engineering, recognized from Clarivate Analytics as Web-of-Science Highly-Cited Researcher in the eight consecutive years 2015-2022.

Prof. Karagiannidis is one of the highly-cited authors across all areas of Electrical Engineering, recognized from Clarivate Analytics as Web-of-Science Highly-Cited Researcher in the eight consecutive years 2015-2022.